An Inverse U-Shaped Curve of Resting-State Networks in Individuals at High Risk of Alzheimer's Disease

Qing Ye, MD[a]; Haifeng Chen, MA[a]; Fan Su, MD[a]; Hao Shu, MD[a]; Liang Gong, MD[a]; Chunming Xie, MD[a]; Hong Zhou, MD[a]; and Feng Bai, MD[a,*]

ABSTRACT

Objective: Higher functional connectivity (FC) in resting-state networks has been shown in individuals at risk of Alzheimer's disease (AD) by many studies. However, the longitudinal trajectories of the FC remain unknown. The present 35-month follow-up study aimed to explore longitudinal changes in higher FC in multiple resting-state networks in subjects with the apolipoprotein E ε4 allele (*ApoE4*) and/or amnestic mild cognitive impairment (aMCI).

Methods: Fifty-one subjects with aMCI and 64 cognitively normal (CN) subjects underwent neuropsychological tests and resting-state functional magnetic resonance imaging (fMRI) scans twice from April 2011 to June 2015. Subjects were divided into 4 groups according to diagnosis and *ApoE4* status. The CN non-*ApoE4* group served as a control group, and other groups served as AD risk groups. The cross-sectional and longitudinal patterns of multiple resting-state networks, including default mode network, hippocampus network, executive control network, and salience network, were explored by comparing FC data between groups and between time points, respectively.

Results: At baseline, compared with the control group, the AD risk groups showed higher FC with 8 regions in multiple networks. At follow-up, 6 of the regions displayed longitudinally decreased FC in AD risk groups. In contrast, the FC with all of these regions was maintained in the control group. Notably, among the 3 risk groups, most of the higher FC at baseline (5 of the 8 regions) and longitudinally decreased FC at follow-up (4 of the 6 regions) were shown in the aMCI *ApoE4* group.

Conclusions: Higher resting-state FC is followed by a decline in subjects at AD risk, and this inverse U-shaped trajectory is more notable in subjects with higher risk.

J Clin Psychiatry 2018;79(2):17m11583

To cite: Ye Q, Chen H, Su F, et al. An inverse U-shaped curve of resting-state networks in individuals at high risk of Alzheimer's disease. *J Clin Psychiatry*. 2018;79(2):17m11583.

To share: https://doi.org/10.4088/JCP.17m11583

[a]Department of Neurology, Affiliated ZhongDa Hospital, School of Medicine, Southeast University, Nanjing, China

*Corresponding author: Feng Bai, MD, Department of Neurology, Affiliated ZhongDa Hospital, School of Medicine, Southeast University, Nanjing, Jiangsu Province, 210009, China (baifeng515@126.com).

Alzheimer's disease (AD) is the most common form of dementia characterized by progressive cognitive impairments and behavioral deficits. The AD pathology begins decades before the onset of dementia,[1] and populations at high risk of AD have gained much attention for AD research. Mild cognitive impairment (MCI) has been considered as a transitional state between normal aging and early AD.[2] MCI confers a high rate of conversion to AD at 10%–15% per year.[3] Individuals carrying the ε4 allele of the apolipoprotein E gene (*ApoE4*), a major genetic risk factor for AD, are also at increased risk of AD,[4] and the presence of both MCI and *ApoE4* is associated with a much greater risk for developing AD.[5,6]

Using resting-state functional magnetic resonance imaging (fMRI) technology, a series of resting-state functional networks have been defined on the basis of the temporal correlations between intrinsic fluctuations of blood oxygen level–dependent signals across functionally related areas, also known as functional connectivity (FC).[7] Disruptions of brain networks, including the default mode network (DMN), the hippocampus network, the executive control network (ECN), and the salience network (SN), have gained major focus because abnormal patterns in these networks were observed in AD patients, MCI subjects, and healthy subjects at risk of AD.[8–13] In addition to extensively decreased FC, subjects at risk of AD also display increased FC, including increased DMN FC with frontal cortex and the hippocampus,[14] increased hippocampus FC with extensive cerebral cortex,[9,15,16] increased ECN FC with frontal cortex and parietal cortex,[17,18] and increased SN FC with cingulate cortex, frontal cortex, insula, and parietal cortex.[19,20] Interestingly, a recent study performed on transgenic mouse models of amyloidosis found that hypersynchrony of resting-state FC was due to early amyloid-beta (Aβ) pathology and followed by hyposynchronized FC at a later period.[21] However, whether the increased FC in subjects at risk of AD is followed by a decline remains relatively unknown.

The present longitudinal resting-state fMRI study recruited cognitively normal (CN) subjects and subjects with amnestic MCI (aMCI, a subtype of MCI characterized by episodic memory loss). According to *ApoE* status, the subjects were further divided into CN non-*ApoE4* group, CN *ApoE4* group, aMCI non-*ApoE4* group, and aMCI *ApoE4* group. The CN non-*ApoE4* group served as a control group, and the other groups served as AD risk groups. Among the 3 risk groups, the aMCI *ApoE4* group was considered at the highest risk for AD. First, the present study analyzed the baseline FC data of

Clinical Points

- Although many studies have shown higher functional connectivity in resting-state networks in individuals at risk of Alzheimer's disease, the longitudinal trajectories of the higher functional connectivity remain relatively unknown.
- The inverse U-shaped trajectories of resting-state functional connectivity found in subjects at risk of Alzheimer's disease may be of value for prediction, identification, and assessment of the disorder.

resting-state networks, including anterior and posterior DMN, hippocampus network, ECN, and SN, between AD risk groups and the control group and detected brain regions showing higher FC in AD risk groups relative to the control group. After nearly 3 years, we then explored the longitudinal changes of the higher FC in these regions. We hypothesized that regions showing higher FC in AD risk groups at baseline would display declines in FC strength during follow-up period and this changing pattern would be most notable in the aMCI *ApoE4* group, which has highest risk for AD.

METHODS

Participants

As described in our prior report,[22] the present study was carried out in accordance with the latest version of the Declaration of Helsinki from April 2011 to June 2015 and was approved by the Affiliated ZhongDa Hospital of Southeast University Research Ethics Committee. Chinese Han participants were recruited by media advertisements and community health screening. Written informed consent was provided by each participant. All subjects underwent a standardized diagnostic evaluation, including demographic information, medical history, and an examination of neurologic status. We initially recruited 87 subjects with aMCI and 135 CN subjects. During the follow-up period, 36 subjects with aMCI were lost due to the development of neurologic or other psychiatric diseases, moves to other cities, being nonresponders, dying, and subjective unwillingness. The follow-up of CN subjects was paused after comparable numbers of subjects with aMCI and CN subjects returned. A total of 51 subjects with aMCI and 64 CN subjects underwent resting-state fMRI scans and neuropsychological tests at both baseline and follow-up. The mean follow-up period was 35 months. Seven subjects with aMCI and 4 CN subjects were excluded after the evaluation of head motion artifacts. Finally, both the aMCI and CN groups were divided into subgroups according to *ApoE* status: the remaining 44 subjects with aMCI were divided into 16 ε4 carriers (aMCI *ApoE4* group) and 28 non-carriers (aMCI non-*ApoE4* group), and the remaining 60 CN subjects were divided into 10 ε4 carriers (CN *ApoE4* group) and 50 non-carriers (CN non-*ApoE4* group). These groups were matched for the duration of the follow-up period (Table 1).

Neuropsychological Assessments

As described previously, each subject underwent a neuropsychological test battery,[23–27] which is described in detail in eAppendix 1.

Inclusion and Exclusion Criteria

Subjects with aMCI were included according to the diagnostic criteria proposed by Petersen[2] and others,[28] which were also described in our prior study.[22] See eAppendix 1 for details on inclusion and exclusion criteria, *ApoE* genotyping, MRI procedures, and image processing. Since global signal has recently been found to be associated with major neuronal components,[29–31] global signal was not regressed out in the present study.

Functional Connectivity Analysis

Seed-based FC analysis was used to construct resting-state networks. Five-mm radius spheres centered at posterior cingulate cortex (PCC) (Montreal Neurologic Institute [MNI] space: −2, −45, 34),[31] medial prefrontal cortex (MNI space: −1, 57, 10),[32] bilateral orbital frontoinsula (MNI space: −38, 26, −10/38, 26, −10),[33] and bilateral dorsolateral prefrontal cortex (MNI space: −42, 34, 20/44, 36, 20)[34,35] served as seed regions for posterior DMN, anterior DMN, bilateral SN, and bilateral ECN, respectively. Bilateral hippocampus regions defined through the automated anatomic labeling template served as seed regions for bilateral hippocampus networks.[36] See eAppendix 1 for more details.

Statistical Analysis

Demographic and neuropsychological data. One-way analysis of variance (ANOVA) and χ^2 tests (applied only in the comparisons of sex) were used to compare the demographic data and neuropsychological performances, respectively, among the 4 groups with significance at $P < .05$. A 2-sample t test and χ^2 tests were used in comparisons of the demographic data between included subjects and excluded subjects with statistically significant differences ($P < .05$). All statistical procedures utilized the SPSS 19.0 software (IBM).

Functional connectivity analysis. To analyze the group differences of each network at baseline, a whole-brain voxel-wise 1-way analysis of covariance was performed on the baseline-stage FC data, controlling for age, sex, and number of years of education (using Resting State fMRI Data Analysis Toolkit [REST] 1.7, REST-Group). The thresholds were set at a corrected $P < .05$, determined by Monte Carlo simulation for multiple comparisons (voxel-wise $P < .05$, FWHM = 6 mm, cluster size > 4,131 mm^3). Then, the average FC strength in each region with significant group differences was extracted in each group at both baseline and follow-up. To detect the higher FC in AD risk groups, a post hoc test (1-way ANOVA) was performed to compare the FC data in each region between the control group and AD risk groups at baseline (using the SPSS 19.0 software). Finally, to explore the longitudinal FC changing patterns in these regions during follow-up, a paired t test was applied in

Table 1. Demographic and Neuropsychological Data[a,b]

Item	CN Non-*ApoE4* (n = 50)	CN *ApoE4* (n = 10)	aMCI Non-*ApoE4* (n = 28)	aMCI *ApoE4* (n = 16)	*F* or χ^2	*P* Value
Age, y	69.54 ± 5.88	68.10 ± 5.43	67.43 ± 6.85	69.25 ± 7.33	0.73	.54
Education, y	12.65 ± 3.18	13.60 ± 2.07	12.02 ± 3.62	12.41 ± 3.45	0.62	.61
Sex, male/female, n	21/29	5/5	18/10	10/6	4.42	.22
Follow-up duration, d	1,029.44 ± 97.25	1,111.20 ± 146.70	1,025.96 ± 154.71	1,083.44 ± 241.55	1.37	.26
MMSE score						
Baseline	28.30 ± 1.36	28.30 ± 1.25	27.39 ± 1.65*	26.33 ± 3.27*,†	5.19	< .01
Follow-up	28.14 ± 1.62	28.30 ± 1.25	27.12 ± 2.05	24.47 ± 5.08*,†,#	8.84	< .01
AVLT-DR score						
Baseline	7.50 ± 1.67	7.20 ± 1.81	3.23 ± 1.27*,†	2.14 ± 1.56*,†,#	69.7	< .01
Follow-up	6.20 ± 1.98	6.00 ± 1.56	2.54 ± 2.23*,†	2.07 ± 2.56*,†	26.25	< .01
CFT score						
Baseline	34.32 ± 1.68	34.50 ± 1.58	33.81 ± 2.12	33.71 ± 2.49	0.75	.53
Follow-up	23.25 ± 7.57	22.60 ± 6.94	32.29 ± 7.00*,†	30.29 ± 6.90*,†	11.03	< .01
CFT-DR score						
Baseline	19.40 ± 5.79	16.45 ± 3.72	14.75 ± 5.47*	10.18 ± 6.09*,†,#	11.31	< .01
Follow-up	21.76 ± 7.01	20.65 ± 5.21	14.63 ± 5.38*,†	12.61 ± 10.16*	9.86	< .01
TMT-A (seconds)						
Baseline	70.38 ± 22.60	55.70 ± 16.07	76.38 ± 22.97†	79.38 ± 17.46†	2.86	.04
Follow-up	73.14 ± 23.25	59.40 ± 16.08	89.54 ± 26.20*,†	87.23 ± 22.10†	5.63	< .01
TMT-B (seconds)						
Baseline	186.60 ± 82.03	159.40 ± 40.49	237.73 ± 97.53*,†	225.54 ± 69.82†	3.48	.02
Follow-up	174.14 ± 54.18	162.70 ± 42.25	234.96 ± 82.23*,†	250.69 ± 129.08	6.73	< .01
CDT score						
Baseline	9.04 ± 1.16	9.30 ± 1.06	8.65 ± 1.50	7.86 ± 1.29*,†	3.83	.01
Follow-up	8.72 ± 1.50	8.90 ± 0.99	8.19 ± 1.60	8.21 ± 1.93	1.04	.38

[a]Values are presented as mean ± SD unless otherwise noted.
[b]χ^2 Test was applied in the comparisons of sex, and 1-way analysis of variance was applied in the other comparisons.
*$P < .05$ vs CN non-*ApoE4* group.
†$P < .05$ vs CN *ApoE4* group.
#$P < .05$ vs aMCI non-*ApoE4* group.
Abbreviations: aMCI = amnestic mild cognitive impairment, *ApoE4* = apolipoprotein E ε4, AVLT-DR = Auditory Verbal Learning Test–Delayed Recall, CDT = Clock Drawing Test, CFT = Rey-Osterrieth Complex Figure Test, CFT-DR = CFT–Delayed Recall, CN = cognitively normal, MMSE = Mini-Mental State Examination, TMT-A and TMT-B = Trail Making Tests A and B.

comparisons of FC between baseline and follow-up in each group. The significance level for post hoc tests was set at $P < .05$.

RESULTS

Demographic and Neuropsychological Data

As shown in Table 1, there was no significant demographic difference among the 4 groups. Both the CN non-*ApoE4* group and the CN *ApoE4* group had results within normal limits on all cognitive tests at both baseline and follow-up. The 2 aMCI groups showed poorer performances in episodic memory tests, including the Auditory Verbal Learning Test (AVLT-DR) and Rey-Osterrieth Complex Figure Test–Delayed Recall (CFT-DR), than the control group (ie, the CN non-*ApoE4* group) at both baseline and follow-up. Notably, the aMCI *ApoE4* group displayed the worst performances on the AVLT-DR and CFT-DR at baseline and on the Mini-Mental State Examination at follow-up, suggesting that the coexistence of aMCI and *ApoE4* conferred much greater cognitive deficits. Furthermore, at follow-up, some subjects converted to aMCI subjects (from 4 control subjects), dementia subjects (from 5 aMCI non-*ApoE4* subjects and 11 aMCI *ApoE4* subjects), or CN subjects (from 4 aMCI non-*ApoE4* subjects and 3 aMCI *ApoE4* subjects). Finally, although some subjects were excluded during analyses, no significant demographic difference was found between included subjects and excluded subjects in either the aMCI group or the CN group (Supplementary eTable 1).

Between-Group FC Analyses at Baseline

Posterior default mode network. As shown in Table 2, compared with the control group, the aMCI *ApoE4* group showed higher posterior DMN FC with the right middle occipital gyrus ($P = .041$) and left precentral gyrus and superior temporal gyrus ($P = .015$) (Figure 1A–1C).

Anterior default mode network. As shown in Table 2, compared with the control group, the 3 risk groups displayed no significantly higher anterior DMN FC at baseline (Figure 1F and 1G).

Hippocampus networks. As shown in Table 2, compared with the control group, higher left hippocampus FC with the right middle temporal gyrus ($P < .001$) and the bilateral middle occipital gyrus and calcarine gyrus ($P < .001$) and higher right hippocampus FC with the right fusiform gyrus and cerebellar vermis ($P = .022$) were shown in the aMCI *ApoE4* group (Figure 2A–2E). Higher right hippocampus FC with the left supramarginal gyrus and superior/middle temporal gyrus were shown in the aMCI non-*ApoE4* group ($P = .001$) (Figure 2D and 2F).

Salience network. As shown in Table 2, compared with the control group, the aMCI non-*ApoE4* group displayed higher left SN FC with the right lingual gyrus, fusiform gyrus, and calcarine gyrus ($P = .002$) (Figure 3A and 3B).

Table 2. Brain Network Functional Connectivity Data[a,b]

Network	Regions With Significance at Baseline	CN Non-*ApoE4*		CN *ApoE4*		aMCI Non-*ApoE4*		aMCI *ApoE4*	
		Baseline	Follow-Up	Baseline	Follow-Up	Baseline	Follow-Up	Baseline	Follow-Up
Posterior DMN	Left precentral gyrus and superior temporal gyrus	0.01 ± 0.19	0.06 ± 0.18	−0.04 ± 0.19	0.02 ± 0.13	−0.08 ± 0.20	0.02 ± 0.20	**0.14 ± 0.11***	0.11 ± 0.13
	Right middle occipital gyrus	0.11 ± 0.18	0.14 ± 0.21	0.18 ± 0.13	0.07 ± 0.14	0.02 ± 0.20*	0.09 ± 0.21	**0.20 ± 0.16***	0.07 ± 0.13#
	Bilateral superior frontal gyrus	0.55 ± 0.14	0.53 ± 0.19	0.41 ± 0.15*	0.34 ± 0.21	0.48 ± 0.20	0.47 ± 0.19	0.37 ± 0.17*	0.32 ± 0.20
	Right superior temporal gyrus and rolandic operculum	0.10 ± 0.20	0.14 ± 0.21	0.07 ± 0.11	0.09 ± 0.12	0.00 ± 0.23*	0.07 ± 0.21	0.21 ± 0.16	0.12 ± 0.17
Anterior DMN	Bilateral posterior cingulate cortex and middle cingulate cortex	0.10 ± 0.13	0.09 ± 0.14	−0.03 ± 0.11*	0.03 ± 0.11	0.02 ± 0.11*	0.08 ± 0.09#	0.11 ± 0.11	0.03 ± 0.11
Left Hip	Bilateral middle occipital gyrus and calcarine gyrus	0.20 ± 0.13	0.22 ± 0.16	0.21 ± 0.17	0.20 ± 0.05	0.18 ± 0.13	0.22 ± 0.15	**0.37 ± 0.13***	0.22 ± 0.12#
	Right middle temporal gyrus	0.23 ± 0.13	0.22 ± 0.15	0.23 ± 0.18	0.21 ± 0.07	0.19 ± 0.12	0.23 ± 0.14	**0.38 ± 0.12***	0.24 ± 0.12#
Right Hip	Right fusiform gyrus and cerebellar vermis	0.20 ± 0.19	0.17 ± 0.20	0.16 ± 0.21	0.16 ± 0.13	0.09 ± 0.23*	0.17 ± 0.19#	**0.33 ± 0.19***	0.20 ± 0.16#
	Left supramarginal gyrus and superior/middle temporal gyrus	0.17 ± 0.18	0.19 ± 0.17	0.16 ± 0.14	0.19 ± 0.13	**0.31 ± 0.19***	0.22 ± 0.18#	0.27 ± 0.11	0.22 ± 0.18
Left SN	Right lingual gyrus, fusiform gyrus and calcarine gyrus	0.16 ± 0.17	0.21 ± 0.20	0.11 ± 0.19	0.15 ± 0.12	**0.29 ± 0.21***	0.19 ± 0.14#	0.17 ± 0.14	0.18 ± 0.12
Right SN	Left inferior frontal gyrus and insula	0.21 ± 0.14	0.24 ± 0.19	**0.43 ± 0.15***	0.36 ± 0.27	0.26 ± 0.16	0.21 ± 0.13	0.22 ± 0.16	0.23 ± 0.16
ECN	None								

[a]Values are presented as mean ± SD. Higher FC in AD risk groups relative to control group at baseline appears in bold.
[b]One-way analysis of covariance was applied in the comparisons of baseline data. Paired *t* test was applied in the comparisons between baseline data and follow-up data.
*$P < .05$ vs HC non-*ApoE4* group (control group) at baseline.
#$P < .05$ vs baseline.
Abbreviations: aMCI = amnestic mild cognitive impairment, *ApoE4* = apolipoprotein E ε4, CN = cognitively normal subjects, DMN = default mode network, ECN = executive control network, Hip = hippocampus network, SN = salience network.

The CN *ApoE4* group displayed higher right SN FC with the left inferior frontal gyrus and insula ($P < .001$) (Figure 3C and 3D).

Executive control network. No significant differences in ECN FC were found between the 4 groups at baseline.

Detailed coordinate information on the regions described in these results is available in Supplementary eTable 2.

FC Analyses Between Baseline and Follow-Up

Posterior default mode network. As shown in Table 2, among the regions related to the higher DMN FC seen at baseline, the right middle occipital gyrus showed longitudinally decreased FC in the aMCI *ApoE4* group ($P = .008$) (Figure 1C) at follow-up, and the left precentral gyrus and superior temporal gyrus showed stable FC during follow-up in aMCI *ApoE4* group ($P = .397$) (Figure 1B). The DMN FC with all of these regions remained stable in the control group.

Hippocampus networks. As shown in Table 2, longitudinally decreased FC was shown in all regions related to higher baseline hippocampus FC, including the left supramarginal gyrus and superior/middle temporal gyrus for the aMCI non-*ApoE4* group ($P = .038$) (Figure 2F) and the bilateral middle occipital gyrus and calcarine gyrus ($P = .003$), right middle temporal gyrus ($P = .002$), and right fusiform gyrus and cerebellar vermis ($P = .048$) for aMCI *ApoE4* group (Figure 2B, 2C and 2E). By contrast, hippocampus FC in all of these regions was maintained in the control group.

Salience network. Among the regions related to higher baseline SN FC, the right lingual gyrus, fusiform gyrus, and calcarine gyrus displayed longitudinally decreased FC in the aMCI non-*ApoE4* group ($P = .045$) (Figure 3B), and the left inferior frontal gyrus and insula displayed stable FC during follow-up in the CN *ApoE4* group ($P = .250$) (Figure 3D). In the control group, the SN FC in all of these regions also remained stable.

In summary, as shown in Table 2, most of the regions (ie, 6 of 8) related to higher baseline FC in AD risk groups displayed longitudinally decreased FC at follow-up. By contrast, in the control group, the FC in all of these regions remained stable. Notably, among the brain networks, the higher FC at baseline was largely related to the hippocampus networks (4 of 8 regions); among the 3 risk groups, most of the higher FC at baseline (5 of 8 regions) and longitudinally

Figure 1. Posterior and Anterior Default Mode Network Functional Connectivity Data[a,b]

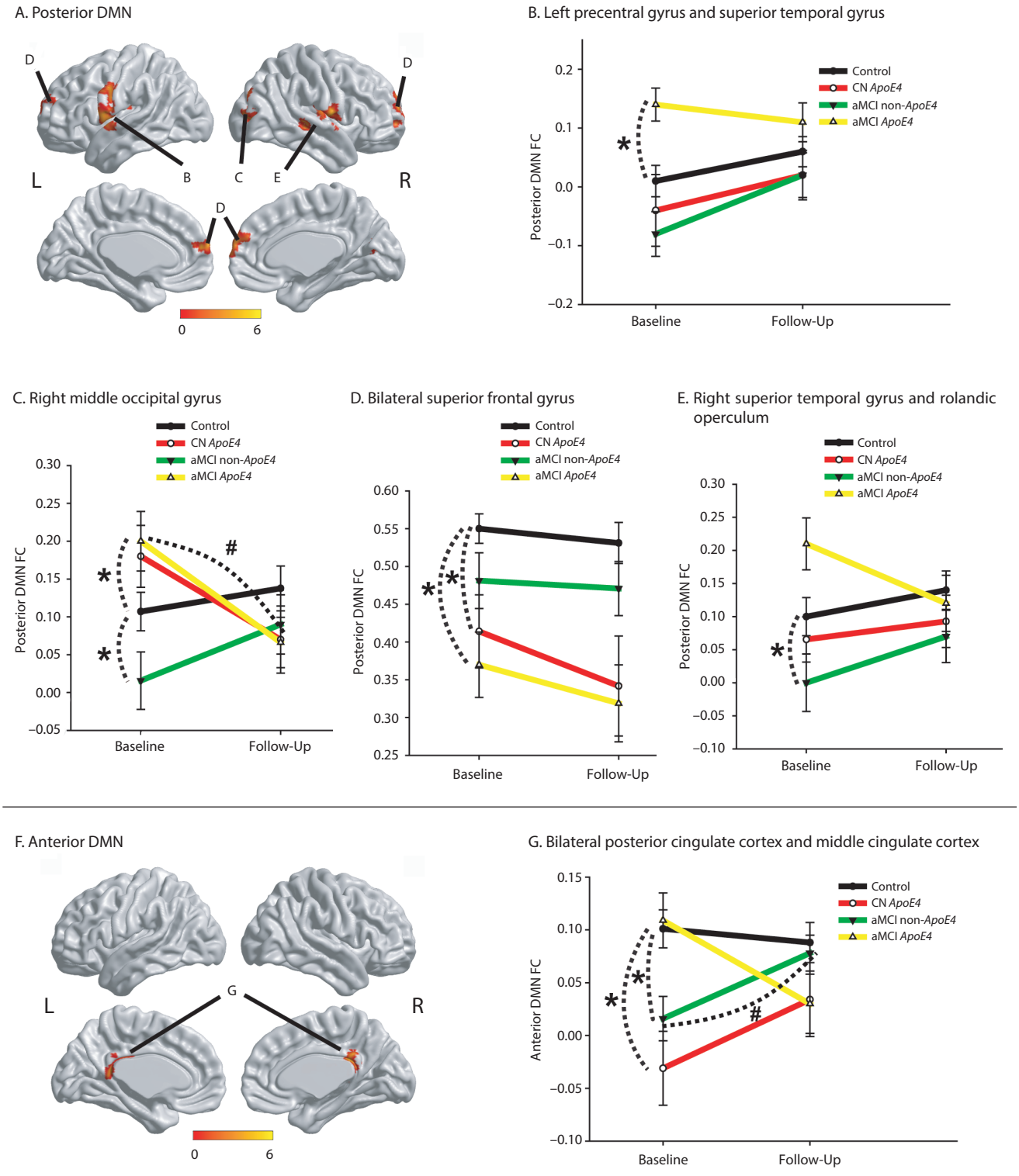

[a](A) Brain regions showing differences of posterior DMN FC among the 4 groups at baseline (groups specified in B, C, D, and E as follows), (B) left precentral gyrus and superior temporal gyrus, (C) right middle occipital gyrus, (D) bilateral superior frontal gyrus, (E) right superior temporal gyrus and rolandic operculum, (F) brain regions showing differences of anterior DMN FC among the 4 groups at baseline (regions specified in G as follows), and (G) bilateral posterior cingulate cortex and middle cingulate cortex.

[b]The spots are presented with *Z* scores. The error bars are presented with standard error. The thresholds were set at a corrected $P < .05$, determined by Monte Carlo simulation for multiple comparisons.

*$P < .05$ vs control group.

#$P < .05$ vs baseline.

Abbreviations: aMCI = amnestic mild cognitive impairment, *ApoE4* = apolipoprotein E ε4, CN = cognitively normal, DMN = default mode network, FC = functional connectivity, L = left, R = right.

Figure 2. Hippocampus Networks Functional Connectivity Data[a,b]

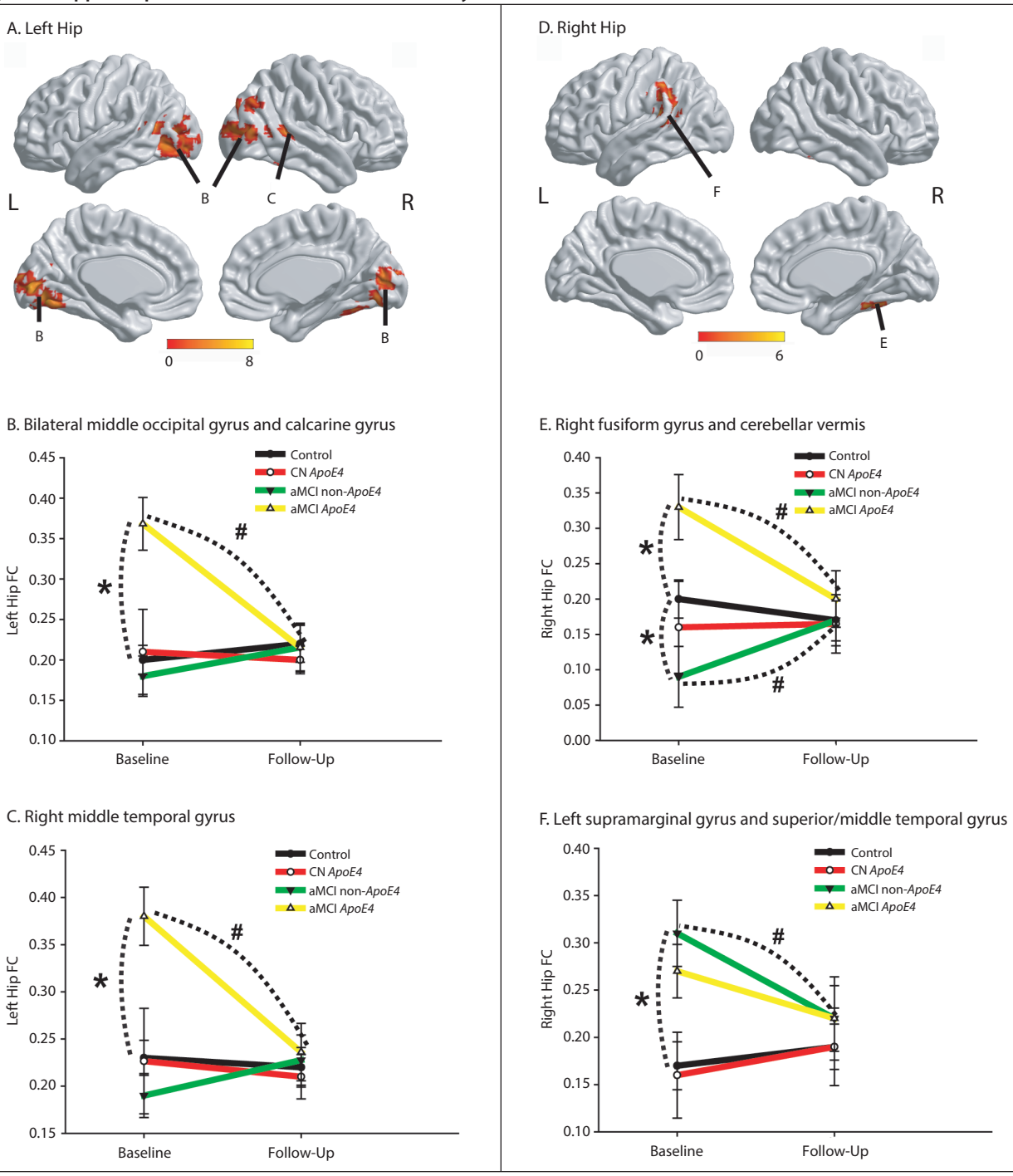

[a](A) Brain regions showing differences of left hippocampus FC among the 4 groups at baseline (groups specified in B and C as follows), (B) bilateral middle occipital gyrus and calcarine gyrus, (C) right middle temporal gyrus, (D) brain regions showing differences of right hippocampus FC among the 4 groups at baseline (regions specified in E and F as follows), (E) right fusiform gyrus and cerebellar vermis, and (F) left supramarginal gyrus and superior/middle temporal gyrus.

[b]The spots are presented with *Z* scores. The error bars are presented with standard error. The thresholds were set at a corrected $P < .05$, determined by Monte Carlo simulation for multiple comparisons.

*$P < .05$ vs control group.

#$P < .05$ vs baseline.

Abbreviations: aMCI = amnestic mild cognitive impairment, *ApoE4* = apolipoprotein E ε4, CN = cognitively normal, FC = functional connectivity. Hip = hippocampus, L = left, R = right.

Figure 3. Salience Network Functional Connectivity Data[a,b]

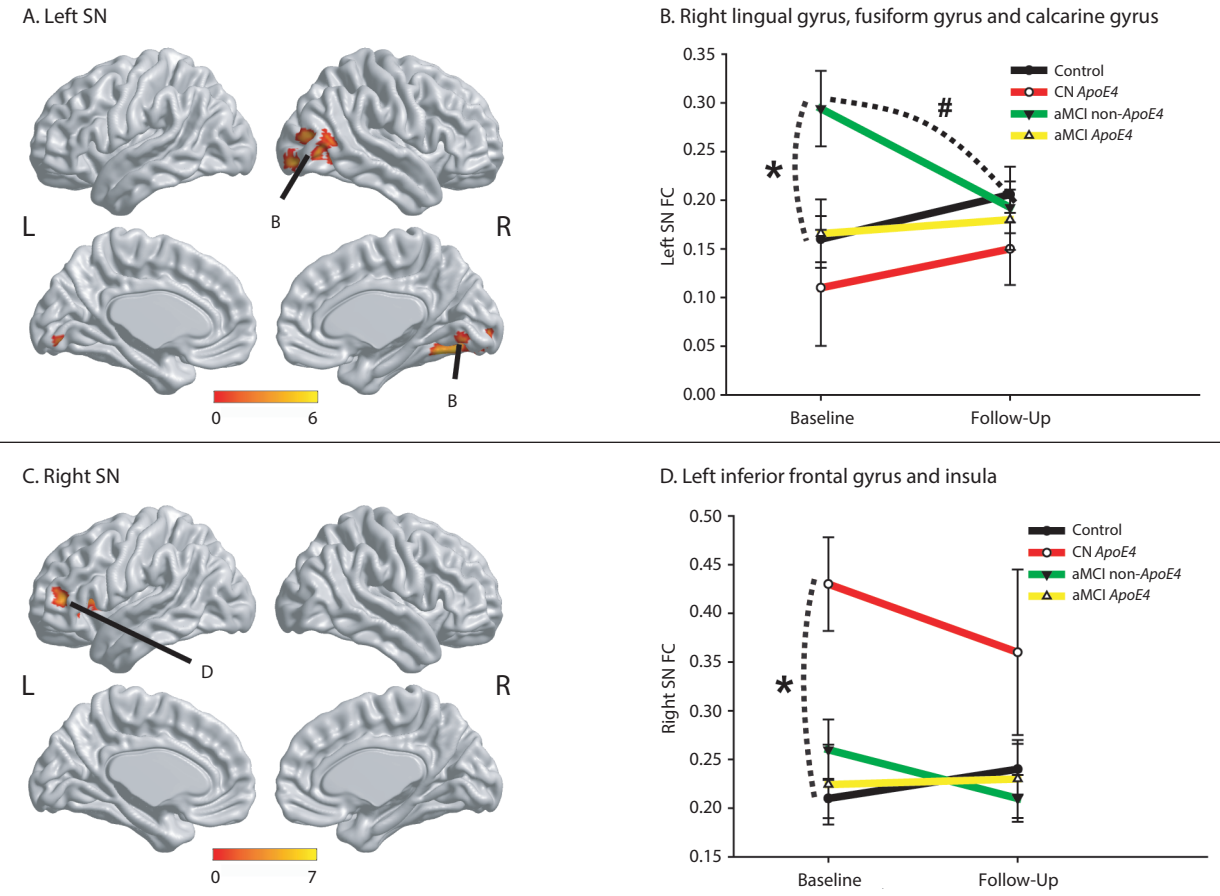

[a](A) Brain regions showing differences of left SN FC among the 4 groups at baseline (groups specified in B as follows); (B) right lingual gyrus, fusiform gyrus, and calcarine gyrus; (C) brain regions showing differences of right SN FC among the 4 groups at baseline (regions specified in D as follows); and (D) left inferior frontal gyrus and insula.

[b]The spots are presented with *Z* scores. The error bars are presented with standard error. The thresholds were set at a corrected $P < .05$, determined by Monte Carlo simulation for multiple comparisons.

*$P < .05$ vs control group.

#$P < .05$ vs baseline.

Abbreviations: aMCI = amnestic mild cognitive impairment, *ApoE4* = apolipoprotein E ε4, CN = cognitively normal, FC = functional connectivity, L = left, R = right, SN = salience network.

decreased FC at follow-up (4 of 6 regions) were shown in the aMCI *ApoE4* group.

In addition, compared with the control group, the 3 risk groups also displayed some regions with lower FC at baseline (Table 2, Figure 1C–1E and 1G, and Figure 2E). During the follow-up period, most of the lower FC at baseline (5 of 7 regions) remained stable.

DISCUSSION

The present study investigated the cross-sectional and longitudinal patterns of brain functional networks in subjects at AD risk. We demonstrated that regions related to higher baseline FC displayed longitudinal decreases of FC at follow-up in subjects at AD risk and that this trajectory was more notable in subjects with higher risk.

The present findings are consistent with a recent study[21] demonstrating that transgenic mouse models of amyloidosis showed increased FC at an early stage but decreased FC at a later stage. That study also suggested that the inverse U-shaped curve of FC was yielded by the development of Aβ pathology. Although the present study did not measure the Aβ pathology by using positron emission tomography imaging or cerebrospinal fluid analyses of Aβ, we divided the subjects into different AD risk groups according to the presence of aMCI and/or *ApoE4*, both of which are associated with the development of Aβ pathology. The Aβ deposition is gradually accelerated during the conversions from normal aging to MCI and from MCI to AD.[37] *ApoE4* carriers exhibit earlier and more abundant Aβ deposition than noncarriers.[38,39] Furthermore, the presence of both aMCI and *ApoE4* is associated with much greater Aβ accumulation.[40] Thus, the aMCI *ApoE4* group in the present study might carry the greatest Aβ accumulation, which might contribute to the most notable inverse U-shaped curve of FC in this group. This inverse U-shaped curve of

FC was also shown by a recent cross-sectional finding that hippocampus FC with frontal and temporal regions initially increased during MCI but then decreased at a later stage.[9]

The mechanisms underlying network hypersynchrony or neuronal hyperactivity have been explored mainly in mouse models of AD. Generally, the hypersynchronized FC or the neuronal hyperactivity is due to the impaired balance between synaptic excitation and inhibition caused by early Aβ development; early Aβ pathology elicits reduced reuptake and enhanced presynaptic release of glutamate[41,42] and reduced GABAergic inhibition,[43] yielding an increased ratio of glutamate/GABA neurotransmitters.[21,44] Then, activated neurons could further release Aβ and cause a vicious cycle that may boost neuronal injuries and synaptic dysfunctions.[44] The vicious cycle may explain the decreases in brain network FC or neuronal activities at later stages of Aβ development.

The present study detected higher FC with extensive regions, including frontal cortex, parietal cortex, temporal cortex, and occipital cortex at baseline. Traditionally, however, hypersynchronized FC or neuronal hyperactivity was found in the frontal and parietal cortex.[45] This increased activity may be because Aβ pathology starts first in the upper neocortex.[46] As the Aβ pathology spreads to the lower parts of the brain,[46] the hypersynchronized FC or neuronal hyperactivity also arises in occipital and temporal regions.[21,47,48] In the present study, the aMCI *ApoE4* group displayed higher FC primarily with temporal and occipital regions, suggesting that the Aβ pathology in this group might have spread to the lower brain regions. By contrast, the CN *ApoE4* group displayed higher FC mainly with the frontal cortex and the aMCI non-*ApoE*4 group displayed higher FC with the parietal, occipital, and temporal cortex, suggesting that the Aβ pathology in the 2 groups might be less severe and involve the upper brain regions, especially in the CN *ApoE4* group. Among the networks, the higher FC was mainly found in the hippocampus networks and related to the occipital and temporal regions. This finding is also consistent with the developing track of Aβ pathology. The hippocampus, occipital cortex, and temporal cortex are affected by Aβ pathology later than the upper neocortex.[46] In the present study, the aMCI subjects with an average age of nearly 70 years might display Aβ deposition in these lower regions, which may contribute to the higher hippocampus FC with the occipital and temporal regions in these subjects. In contrast, the lower FC at baseline in groups at risk for AD was mainly shown in DMN with PCC and medial prefrontal cortex as seeds that are relatively upper regions. The result suggests that the upper brain regions of these subjects might be at a much later stage of Aβ plaque development with severe neuronal injuries and synaptic dysfunctions.

Some limitations should be noted. First, the sample size was small. At follow-up, several subjects converted to MCI subjects, dementia subjects, or CN subjects; however, comparisons between converters and nonconverters could not be performed with the limited sample size. Thus, the conversion effect on FC changes could not be assessed. Due to the small sample size, we did not perform correlation analyses between cognitive function and FC. Second, during the nearly 3-year follow-up, fMRI scans were conducted only twice. Our results confirmed only the decline part of the inverse U-shaped curve of FC. FMRI scans at multiple time points would be helpful for better illustrating the curve. We will continue to follow up with these subjects. Finally, due to the incomplete data about the onset time of subjective memory impairment, we failed to analyze the onset time of the symptoms for aMCI subjects, an analysis that may help to illustrate longitudinal trajectories more accurately.

In conclusion, hypersynchronized FC of resting-state brain networks was followed by a decline in subjects at risk for AD, and the trajectory was more notable in subjects at higher risk. The findings could shed light on aging trajectories of resting-state functional networks in subjects at AD risk. These aging trajectories should be validated with data from a larger sample with long-term follow-up and would be of value for prediction, identification, and assessment of the disorder.

Submitted: March 16, 2017; accepted August 14, 2017.

Published online: February 20, 2018.

Potential conflicts of interest: None.

Funding/support: This research was supported by the National Natural Science Foundation of China (No. 81671665), Jiangsu Provincial Key Medical Talents (No. ZDRCA2016085), and the Natural Science Foundation of Jiangsu Province (No. BK20160071). All grants were awarded to Dr Bai.

Role of the sponsor: The funding source had no role in the study design, data collection, analysis, management, interpretation of the data, or writing of the article.

Acknowledgments: We thank Qin Xu, MA, and Ying Cheng, MA, of Southeast University, for their technical help in fMRI scanning. Neither Ms Xu nor Ms Cheng has any potential conflicts of interest relevant to the subject of this article.

Supplementary material: See accompanying pages.

REFERENCES

1. Jack CR Jr, Knopman DS, Jagust WJ, et al. Tracking pathophysiological processes in Alzheimer's disease: an updated hypothetical model of dynamic biomarkers. *Lancet Neurol*. 2013;12(2):207–216.
2. Petersen RC. Mild cognitive impairment as a diagnostic entity. *J Intern Med*. 2004;256(3):183–194.
3. Petersen RC, Smith GE, Waring SC, et al. Mild cognitive impairment: clinical characterization and outcome. *Arch Neurol*. 1999;56(3):303–308.
4. Strittmatter WJ, Weisgraber KH, Huang DY, et al. Binding of human apolipoprotein E to synthetic amyloid beta peptide: isoform-specific effects and implications for late-onset Alzheimer disease. *Proc Natl Acad Sci U S A*. 1993;90(17):8098–8102.
5. Li JQ, Tan L, Wang HF, et al. Risk factors for predicting progression from mild cognitive impairment to Alzheimer's disease: a systematic review and meta-analysis of cohort studies. *J Neurol Neurosurg Psychiatry*. 2016;87(5):476–484.
6. Elias-Sonnenschein LS, Viechtbauer W, Ramakers IH, et al. Predictive value of APOE-ε4 allele for progression from MCI to AD-type dementia: a meta-analysis. *J Neurol Neurosurg Psychiatry*. 2011;82(10):1149–1156.
7. Damoiseaux JS, Rombouts SA, Barkhof F, et al. Consistent resting-state networks across healthy subjects. *Proc Natl Acad Sci U S A*. 2006;103(37):13848–13853.
8. Joo SH, Lim HK, Lee CU. Three large-scale functional brain networks from resting-state functional MRI in subjects with different levels of cognitive impairment. *Psychiatry Investig*. 2016;13(1):1–7.
9. Sohn WS, Yoo K, Na DL, et al. Progressive changes in hippocampal resting-state connectivity across cognitive impairment: a cross-sectional study from normal to Alzheimer disease. *Alzheimer Dis Assoc Disord*. 2014;28(3):239–246.
10. Wee CY, Yap PT, Zhang D, et al. Identification of MCI individuals using structural and functional

connectivity networks. *Neuroimage*. 2012;59(3):2045–2056.
11. Zhu H, Zhou P, Alcauter S, et al. Changes of intranetwork and internetwork functional connectivity in Alzheimer's disease and mild cognitive impairment. *J Neural Eng*. 2016;13(4):046008.
12. He X, Qin W, Liu Y, et al. Abnormal salience network in normal aging and in amnestic mild cognitive impairment and Alzheimer's disease. *Hum Brain Mapp*. 2014;35(7):3446–3464.
13. Su YY, Zhang XD, Schoepf UJ, et al. Lower functional connectivity of default mode network in cognitively normal young adults with mutation of APP, presenilins and APOE ε4. *Brain Imaging Behav*. 2017;11(3):818–828.
14. Gardini S, Venneri A, Sambataro F, et al. Increased functional connectivity in the default mode network in mild cognitive impairment: a maladaptive compensatory mechanism associated with poor semantic memory performance. *J Alzheimers Dis*. 2015;45(2):457–470.
15. Wang Z, Liang P, Jia X, et al. Baseline and longitudinal patterns of hippocampal connectivity in mild cognitive impairment: evidence from resting state fMRI. *J Neurol Sci*. 2011;309(1-2):79–85.
16. Shu H, Yuan Y, Xie C, et al. Imbalanced hippocampal functional networks associated with remitted geriatric depression and apolipoprotein E ε4 allele in nondemented elderly: a preliminary study. *J Affect Disord*. 2014;164:5–13.
17. Wu L, Soder RB, Schoemaker D, et al. Resting state executive control network adaptations in amnestic mild cognitive impairment. *J Alzheimers Dis*. 2014;40(4):993–1004.
18. Liang P, Wang Z, Yang Y, et al. Three subsystems of the inferior parietal cortex are differently affected in mild cognitive impairment. *J Alzheimers Dis*. 2012;30(3):475–487.
19. Goveas JS, Xie C, Chen G, et al. Functional network endophenotypes unravel the effects of apolipoprotein E epsilon 4 in middle-aged adults. *PLoS One*. 2013;8(2):e55902.
20. Machulda MM, Jones DT, Vemuri P, et al. Effect of APOE ε4 status on intrinsic network connectivity in cognitively normal elderly subjects. *Arch Neurol*. 2011;68(9):1131–1136.
21. Shah D, Praet J, Latif Hernandez A, et al. Early pathologic amyloid induces hypersynchrony of BOLD resting-state networks in transgenic mice and provides an early therapeutic window before amyloid plaque deposition. *Alzheimers Dement*. 2016;12(9):964–976.
22. Ye Q, Su F, Shu H, et al. The apolipoprotein E gene affects the three-year trajectories of compensatory neural processes in the left-lateralized hippocampal network. *Brain Imaging Behav*. 2017;11(5):1446–1458.
23. Folstein MF, Folstein SE, McHugh PR. "Mini-mental state": a practical method for grading the cognitive state of patients for the clinician. *J Psychiatr Res*. 1975;12(3):189–198.
24. Geffen GM, Butterworth P, Geffen LB. Test-retest reliability of a new form of the Auditory Verbal Learning Test (AVLT). *Arch Clin Neuropsychol*. 1994;9(4):303–316.
25. Boone KB. The Boston Qualitative Scoring System for the Rey-Osterrieth Complex Figure. *J Clin Exp Neuropsychol*. 2000;22(3):430–434.
26. Hooper SR. Review of *A Compendium of Neuropsychological tTests: Administration, Norms, and Commentary*, 2nd ed. *Contemporary Psychology: APA Review of Books*. 1999;44(6):491–493.
27. Sunderland T, Hill JL, Mellow AM, et al. Clock drawing in Alzheimer's disease: a novel measure of dementia severity. *J Am Geriatr Soc*. 1989;37(8):725–729.
28. Winblad B, Palmer K, Kivipelto M, et al. Mild cognitive impairmen—-beyond controversies, towards a consensus: report of the International Working Group on Mild Cognitive Impairment. *J Intern Med*. 2004;256(3):240–246.
29. Guo CC, Kurth F, Zhou J, et al. One-year test-retest reliability of intrinsic connectivity network fMRI in older adults. *Neuroimage*. 2012;61(4):1471–1483.
30. Hahamy A, Calhoun V, Pearlson G, et al. Save the global: global signal connectivity as a tool for studying clinical populations with functional magnetic resonance imaging. *Brain Connect*. 2014;4(6):395–403.
31. Shu H, Shi Y, Chen G, et al. Opposite neural trajectories of apolipoprotein E ϵ4 and ϵ2 alleles with aging associated with different risks of Alzheimer's disease. *Cereb Cortex*. 2016;26(4):1421–1429.
32. Bado P, Engel A, de Oliveira-Souza R, et al. Functional dissociation of ventral frontal and dorsomedial default mode network components during resting state and emotional autobiographical recall. *Hum Brain Mapp*. 2014;35(7):3302–3313.
33. Elton A, Gao W. Divergent task-dependent functional connectivity of executive control and salience networks. *Cortex*. 2014;51:56–66.
34. Ham JH, Cha J, Lee JJ, et al. Nigrostriatal dopamine-independent resting-state functional networks in Parkinson's disease. *Neuroimage*. 2015;119:296–304.
35. Seeley WW, Menon V, Schatzberg AF, et al. Dissociable intrinsic connectivity networks for salience processing and executive control. *J Neurosci*. 2007;27(9):2349–2356.
36. Tzourio-Mazoyer N, Landeau B, Papathanassiou D, et al. Automated anatomical labeling of activations in SPM using a macroscopic anatomical parcellation of the MNI MRI single-subject brain. *Neuroimage*. 2002;15(1):273–289.
37. Saido TC. Metabolism of amyloid β peptide and pathogenesis of Alzheimer's disease. *Proc Jpn Acad, Ser B, Phys Biol Sci*. 2013;89(7):321–339.
38. Morishima-Kawashima M, Oshima N, Ogata H, et al. Effect of apolipoprotein E allele epsilon4 on the initial phase of amyloid beta-protein accumulation in the human brain. *Am J Pathol*. 2000;157(6):2093–2099.
39. Morris JC, Roe CM, Xiong C, et al. APOE predicts amyloid-beta but not tau Alzheimer pathology in cognitively normal aging. *Ann Neurol*. 2010;67(1):122–131.
40. Bangen KJ, Clark AL, Werhane M, et al; Alzheimer's Disease Neuroimaging Initiative. Cortical amyloid burden differences across empirically-derived mild cognitive impairment subtypes and interaction with APOE E4 genotype. *J Alzheimers Dis*. 2016;52(3):849–861.
41. Li S, Hong S, Shepardson NE, et al. Soluble oligomers of amyloid beta protein facilitate hippocampal long-term depression by disrupting neuronal glutamate uptake. *Neuron*. 2009;62(6):788–801.
42. Fogel H, Frere S, Segev O, et al. APP homodimers transduce an amyloid-β-mediated increase in release probability at excitatory synapses. *Cell Reports*. 2014;7(5):1560–1576.
43. Verret L, Mann EO, Hang GB, et al. Inhibitory interneuron deficit links altered network activity and cognitive dysfunction in Alzheimer model. *Cell*. 2012;149(3):708–721.
44. Busche MA, Konnerth A. Neuronal hyperactivity—a key defect in Alzheimer's disease? *BioEssays*. 2015;37(6):624–632.
45. Spaniol J, Grady C. Aging and the neural correlates of source memory: over-recruitment and functional reorganization. *Neurobiol Aging*. 2012;33(2):425.e3–425.e18.
46. Thal DR, Rüb U, Orantes M, et al. Phases of A beta-deposition in the human brain and its relevance for the development of AD. *Neurology*. 2002;58(12):1791–1800.
47. Busche MA, Chen X, Henning HA, et al. Critical role of soluble amyloid-β for early hippocampal hyperactivity in a mouse model of Alzheimer's disease. *Proc Natl Acad Sci U S A*. 2012;109(22):8740–8745.
48. Grienberger C, Rochefort NL, Adelsberger H, et al. Staged decline of neuronal function in vivo in an animal model of Alzheimer's disease. *Nat Commun*. 2012;3:774.

Supplementary material follows this article.

THE JOURNAL OF CLINICAL PSYCHIATRY
THE OFFICIAL JOURNAL OF THE AMERICAN SOCIETY OF CLINICAL PSYCHOPHARMACOLOGY

Supplementary Material

Article Title: An Inverse U-Shaped Curve of Resting-State Networks in Individuals at High Risk of Alzheimer's Disease

Author(s): Qing Ye, MD[a]; Haifeng Chen, MA[a]; Fan Su, MD[a]; Hao Shu, MD[a]; Liang Gong, MD[a]; Chunming Xie, MD[a]; Hong Zhou, MD[a]; and Feng Bai, MD[a,*]

DOI Number: https://doi.org/10.4088/JCP.17m11583

List of Supplementary Material for the article

1. **eAppendix 1** Materials and Methods
2. **eTable 1** Demographic data of included subjects and excluded subjects
3. **eTable 2** Brain regions with significance at baseline

Disclaimer

This Supplementary Material has been provided by the author(s) as an enhancement to the published article. It has been approved by peer review; however, it has undergone neither editing nor formatting by in-house editorial staff. The material is presented in the manner supplied by the author.

eAppendix 1

1. Materials and methods

1.1. Neuropsychological assessments

Global cognitive function was assessed by a Mini Mental State Examination (MMSE), a Clinical Dementia Rating (CDR) and a Mattis Dementia Rating Scale-2 (MDRS-2). All subjects underwent a neuropsychological battery test including an auditory-verbal learning test-delayed recall (AVLT-DR), Rey-Osterrieth complex figure test (CFT) with its 20-min delayed recall (CFT-DR), clock drawing test (CDT), and trail making tests (TMT)-A and B.

1.2. Inclusion and exclusion criteria

The inclusion criteria of aMCI were as follows: 1) subjective memory impairment corroborated by the subject and an informant, 2) objective memory performances documented by an AVLT-DR score ≤ 1.5 standard deviations of education-adjusted and age-adjusted norms (the cutoff was ≤ 4 correct responses on 12 items for ≥ 8 years of education), 3) normal general cognitive function evaluated by an MMSE score ≥ 24, 4) a CDR of 0.5, with at least a 0.5 in the memory domain, 5) minimal or no impairment of routine daily life activities, 6) the absence of dementia or insufficiency in meeting the National Institute of Neurological and Communicative Disorders and Stroke and the AD and Related Disorders Association (NINCDS-ADRDA) and DSM-IV criteria for AD. Exclusion criteria were as follows: 1) a history of alcoholism, stroke (modified Hachinski score of > 4), Parkinson's disease, head injury, major depression (excluded by a self-rating depression scale), epilepsy,

or other neurological or psychiatric illness (excluded by clinical assessment and case history), 2) major medical illness (e.g., anemia, cancer, and thyroid dysfunction), 3) severe hearing or visual loss, 4) T2-weighted MRI displaying infarction, major white matter changes, or other lesions (two experienced radiologists executed the scans). Control subjects were required to have a clinical dementia rating of 0, an MMSE score of ≥ 26, and a delayed recall score of > 4 for those with ≥ 8 years of education. The inclusion and exclusion assessments were conducted by 2 experienced neuropsychiatric physicians who administered a structured interview to subjects and their informants.

1.3. ApoE genotyping

Genomic DNA was extracted from 250 μL EDTA-anticoagulated blood collected from each subject using a DNA direct kit (Tiangen, China). A polymerase chain reaction-based restriction fragment length polymorphism (PCR-RFLP) assay was employed to detect the rs7412 and rs429358 alleles, the haplotype of which ultimately determined the *ApoE* genotype.

1.4. Magnetic resonance imaging procedures

All subjects were scanned using a Siemens Verio 3.0-T scanner (Siemens, Erlangen, Germany) with a 12-channel head coil at the Affiliated ZhongDa Hospital of Southeast University. The subjects were told to keep their eyes closed and relax during the scan. Their ears were occluded with earplugs, and their heads were immobilized using foam pads and belts to minimize head motion. Resting-state functional images, including 240 volumes, were acquired by a gradient-recalled echo-

planar imaging (GRE-EPI) sequence: repetition time (TR) = 2000 ms; flip angle (FA) = 90°; echo time (TE) = 25 ms; field of view (FOV) = 240 × 240 mm; acquisition matrix = 64 × 64; gap = 0 mm; thickness = 4.0 mm; number of slices = 36. High-resolution T1-weighted axial images covering the whole brain were obtained by a 3D-magnetization prepared rapid gradient-echo sequence: TR = 1900 ms; FA = 9°; TE = 2.48 ms; FOV = 250 × 250 mm; acquisition matrix = 256 × 256; gap = 0 mm, thickness = 1.0 mm; number of slices = 176. Additionally, routine axial T2-weighted images were obtained to exclude subjects with major white matter changes, cerebral infarction, or other lesions.

1.5. Image preprocessing

Imaging data were analyzed using Data Processing Assistant for Resting-State fMRI (DPARSF) V2.1 (http://www.restfmri.net/forum/DPARSF). The first 10 volumes of the scanning session were discarded to allow for T1 equilibration effects. Then, the slice timing and realignment procedures were performed to correct for the time differences in acquisition among slices within one volume, and the motion effects (6-parameter rigid body) during the scan. Participants with head motion > 3 mm in transition or 3° in rotation were excluded. The resulting images were spatially normalized into a standard stereotaxic space with a 12-parameter affine approach and an EPI template image, and then resampled to 3 × 3 × 3 mm voxels, and smoothed with a Gaussian kernel of 6 × 6 × 6 mm. Finally, white matter, cerebrospinal fluid and 6 head motion parameters were removed as covariates of no interest.

1.6. FC analysis

For each subject, a mean time series of each seed region was computed as the reference time course for each network. Pearson cross-correlation analysis was performed between the seed time course and the time course of the whole-brain voxels. A Fisher's *z*-transformation was applied to improve the normality of the correlation coefficients $z = 0.5 \times \ln \frac{1+\mathrm{r}}{1-\mathrm{r}}$. Finally, the individual maps of each network were obtained.

Supplementary eTable 1 Demographic data of included subjects and excluded subjects[a,b]

Items	aMCI				cognitive normal			
	Included subjects (*n* = 44)	Excluded subjects (*n* = 43)	*t* or χ^2	*P*-value	Included subjects (*n* = 60)	Excluded subjects (*n* = 75)	*t* or χ^2	*P*-value
Age (years)	68.09±7.00	71.00±7.66	−1.85	0.07	69.30±5.79	67.45±7.22	1.65	0.1
Education (years)	12.16±3.52	11.49±2.79	0.98	0.33	12.81±3.03	11.85±3.06	1.81	0.07
Gender (male: female)	28:16	19:24	3.31	0.07	26:34	39:36	1	0.32

[a]Values are presented as the mean ± stand deviation (SD).

[b]χ^2 test was applied in the comparisons of gender and a two-sample *t* test was applied in the other comparisons.

Supplementary eTable 2 Brain regions with significance at baseline[a]

Network	Brain region	BA	Peak MNI coordinates x, y, z (mm)	Peak F value	Cluster size (mm^3)
Posterior DMN					
	Left precentral gyrus and superior temporal gyrus	4, 48	−57, −1, 1	4.44	4590
	Right middle occipital gyrus	19	21, −75, 15	5.55	4158
	Bilateral superior frontal gyrus	10	−12, 57, 18	5.33	4293
	Right superior temporal gyrus and rolandic operculum	48	57, −6, 12	4.81	4212
Anterior DMN					
	Bilateral posterior cingulate cortex and middle cingulate cortex	26, 29	8, −35, 14	5.9	10395
Left Hip					
	Bilateral middle occipital gyrus and calcarine gyrus	17, 18, 19	−27, −78, −3	7.84	54891
	Right middle temporal gyrus	21, 37	45, −42, 6	6.06	4833
Right Hip					
	Right fusiform gyrus and cerebellar vermis	37	−3, −45, −39	5.37	6696
	Left supramarginal gyrus and superior/middle temporal gyrus	40, 42	−54, −51, 21	5.28	4563
Left SN					
	Right lingual gyrus, fusiform gyrus and calcarine gyrus	18, 19	24, −84, −3	5.82	12825
Right SN					
	Left inferior frontal gyrus and insula	45, 46, 48	−40, 38, 1	6.69	4860
ECN					
	None				

[a]The thresholds were set at a corrected $P < 0.05$, determined by Monte Carlo simulation for multiple comparisons.

Abbreviations: BA = Brodmann's area, MNI = Montreal Neurological Institute, DMN = default mode network, Hip = hippocampus network, SN = salience network, ECN = executive control network.